

# 000 SPEAK TO A PROTEIN: AN INTERACTIVE MULTIMODAL 001 CO-SCIENTIST FOR PROTEIN ANALYSIS

002  
003  
004  
005 **Anonymous authors**  
006 Paper under double-blind review

## 007 008 ABSTRACT

009  
010  
011 Building a working mental model of a protein typically requires weeks of reading, cross-  
012 referencing crystal and predicted structures, and inspecting ligand complexes, an effort  
013 that is slow, unevenly accessible, and often requires specialized computational skills.  
014 We introduce *Speak to a Protein*, a new capability that turns protein analysis into an  
015 interactive, multimodal dialogue with an expert co-scientist. The AI system retrieves  
016 and synthesizes relevant literature, structures, and ligand data; grounds answers in a  
017 live 3D scene; and can highlight, annotate, manipulate and see the visualization. It  
018 also generates and runs code when needed, explaining results in both text and graph-  
019 ics. We demonstrate these capabilities on relevant proteins, posing questions about bind-  
020 ing pockets, conformational changes, or structure-activity relationships to test ideas in  
021 real-time. *Speak to a Protein* reduces the time from question to evidence, lowers the  
022 barrier to advanced structural analysis, and enables hypothesis generation by tightly  
023 coupling language, code, and 3D structures. *Speak to a Protein* is freely accessible at  
024 <https://www.anonymousplayground.com>.

025 **Keywords** Agentic co-scientist, scientific discovery, molecular visualization, deep research, drug discov-  
026 ery, retrieval-augmented generation

## 027 1 INTRODUCTION

028  
029 Proteins are the molecular machinery of life, and understanding their structure and function is fundamental  
030 to modern biology and medicine. For a researcher in drug discovery or molecular biology, developing an  
031 intuitive, "working mental model" of a target protein, its active sites, its conformational dynamics, and its  
032 network of interactions is a critical first step. However, this process is slow and arduous, often requiring a  
033 combination of deep domain knowledge and specialized computational skills.

034  
035 A researcher investigating a protein kinase to understand how a new series of inhibitors might bind must  
036 embark on a fragmented and technically demanding workflow. This involves sifting through the PubMed  
037 literature (Sayers et al., 2020), fetching and comparing multiple structures from the Protein Data Bank  
038 (PDB) (Burley et al., 2018), querying UniProt (The UniProt Consortium, 2022) for functional annotations  
039 and disease-associated variants, and extracting structure-activity relationship (SAR) data from databases  
040 like ChEMBL (Mendez et al., 2018). Each step requires navigating different interfaces and data formats.  
041 Furthermore, deeper analysis, such as superimposing structures, identifying key interactions, or plotting  
042 bioactivity data, requires proficiency with specialized software or scripting languages, creating a significant  
043 barrier to entry for many bench scientists. This high friction for asking and answering questions restrains  
044 curiosity and slows the pace of discovery.

045 To address these challenges, we introduce *Speak to a Protein*, a new capability designed to transform protein  
046 analysis into an interactive dialogue with an AI co-scientist that collaborates with the user in real-time. Us-  
047 ing recent advances in large language models (LLMs) and their evolution into multimodal scientific agents  
048 (Caffagni et al., 2024; Zhang et al., 2024; Wang et al., 2024b), our system can comprehend complex, natural  
049 language queries about a protein of interest. It autonomously retrieves, integrates, and synthesizes informa-  
050 tion from a comprehensive suite of biological data sources, including literature, structural repositories, and  
051 biochemical databases.

052 The core innovation of *Speak to a Protein* is its ability to ground its responses across multiple, synchronized  
053 modalities. When a user asks a question, the AI does not simply return text. It interacts with a live 3D  
054 structural viewer to highlight residues, measure distances, or annotate binding pockets. It can generate and  
055 execute Python code in a sandboxed environment to perform calculations, filter tabular data, or generate  
056 plots on the fly. Furthermore, the AI co-scientist sees, understands and controls the visualization, offering  
057 a natural interaction with the user. This tight coupling of natural language, 3D visualization, and code  
058 execution creates a seamless and intuitive environment for scientific exploration.

059 This paper makes the following contributions: We present the design and architecture of an AI system that  
060 integrates language, code execution, and 3D visualization for interactive protein analysis. We show how

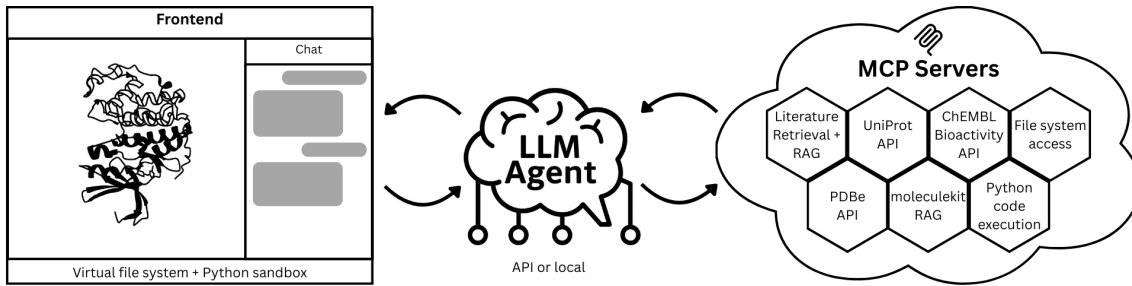


Figure 1: **Overview of the system architecture.** The system consists of a frontend with a protein viewer and chat interface, which includes a virtual file system and Python sandbox for automated code execution and viewer manipulation. The LLM Agent is the main orchestrator that interacts with the user and calls a set of custom tools through Model Context Protocol (MCP). These tools include a literature search for a given protein and text query, retrieving specialized data through APIs such as UniProt, PDBe and ChEMBL, as well as executing Python code in a sandbox environment with a dedicated virtual file system.

this multimodal approach drastically lowers the barrier to complex structural and biochemical data analysis. Through case studies on relevant proteins, we show that this system enables a more fluid and powerful form of hypothesis generation, accelerating the cycle from question to evidence.

## 2 RELATED WORK

The ambition to create an AI capable of scientific discovery is a long-standing goal, articulated in visions such as Hiroaki Kitano’s proposal for an “AI Scientist”: a system that could autonomously formulate hypotheses, design experiments, and achieve Nobel-class discoveries (Kitano, 2021). While such a fully autonomous system (Boiko et al., 2023; Zou et al., 2025) remains a grand challenge, recent progress in large language models (LLMs) has enabled the development of a more immediate and collaborative paradigm: the “AI co-scientist” or “advanced intelligence” in Kitano’s words.

Early systems explored conversational interfaces for structural inspection and Q&A over proteins. Guo et al. (2023) demonstrated *ProteinChat*, which couples LLM prompting with protein 3D structures to answer user questions about residues and pockets. Contemporary efforts such as Wang et al. (2024a) and Xiao et al. (2024) investigate protein-aware prompting and multimodal conditioning for function/property reasoning. Most recently, Wang et al. (2025) proposes *Prot2Chat*, an LLM that fuses protein sequence, structure, and text via an early-fusion adapter, directly targeting protein Q&A.

Beyond text-only chat, domain copilots increasingly drive molecular viewers and modeling tools. Sun et al. (2024) introduce *ChatMol Copilot*, an LLM agent that coordinates cheminformatics and modeling tools (e.g., docking, conformer generation) in response to natural-language requests. In parallel, Ille et al. (2024) systematically evaluates GPT-4’s ability to perform rudimentary structural modeling and protein–ligand interaction analysis, highlighting both promise and limitations. Our work is aligned with this line but centers on tightly coupling language, code execution, and a live 3D scene for grounded, manipulable answers.

Agent frameworks augment LLMs with tool use, retrieval, and planning. *ChemCrow* (Bran et al., 2024) shows that equipping GPT-4 with chemistry tools enables multi-step synthesis planning and materials tasks. More recently, CLADD (Lee et al., 2025) proposes a retrieval-augmented multi-agent system specialized for drug discovery tasks. *Speak to a Protein* adopts the agentic paradigm for structural biology: it retrieves literature/structures, executes analyses (e.g., pocket mapping, SAR tables), and grounds responses in synchronized 3D visualizations.

Compared to prior work, our contribution is an end-to-end, *interactive co-scientist* for proteins that (i) unifies literature/structure/ligand retrieval, (ii) reasons with tabular and 3D modalities, (iii) executes code for on-the-fly analyses, and (iv) directly annotates/manipulates the 3D scene in response to dialogue (Table 1). This tightly coupled language–code–3D loop reduces the time from question to evidence relative to agent-only or text-only systems.

## 3 SYSTEM OVERVIEW: *Speak to a Protein*

### 3.1 ARCHITECTURE

The system architecture of *Speak to a Protein* (Figure 1) is organized around two main components: a front-end for user interaction and visualization, and a back-end for language understanding, tool coordination, and data retrieval. This is effectively a visual channel of communication between the AI co-scientist and the human scientist. The front-end provides the primary user interface, incorporating both a conversational

122 Table 1: Comparison of Speak to a Protein with representative LLM-based systems developed for drug  
 123 discovery, as well as with general-purpose AI models. Speak to a Protein uniquely combines access to mul-  
 124 tiple biological databases, scientific literature extraction, on-the-fly code execution, real-time 3D molecular  
 125 visualization, multimodal reasoning grounded in structural data, and persistent knowledge management.  
 126 These capabilities are not collectively available in other existing platforms.

System	API Access	Lit. Extraction	Code Sandbox	3D Vis. Control	Multimodal Reasoning	Persistent Memory
Speak to a protein	Yes	Yes	Yes	Yes	Yes (Live 3D scene)	Yes
General-purpose AI	Not natively	Partial (cannot retrieve)	Yes	No	No	No
ProteinChat	No	No	No	No	Yes (Structure Description)	No
Prot2Chat	No	No	No	No	Yes (3D/Sequence Fusion)	No
ChatMol Copilot	No	No	No	Yes	Yes (Analyzes structure visualization)	No
ChemCrow	Yes	Yes	Yes	No	No	Yes
CLADD	Yes	Yes	No	No	No	No

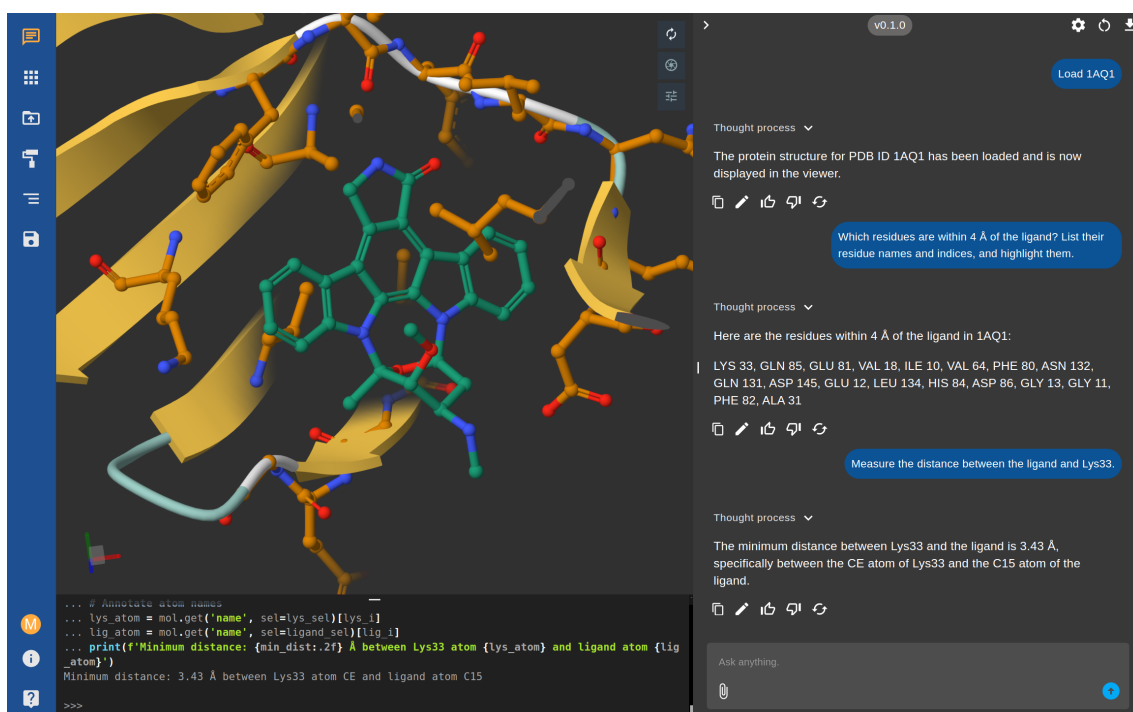


Figure 2: Interactive analysis of the CDK2 structure (PDB: 1AQ1) using the *Speak to a Protein* multimodal assistant. The user enters natural language queries in the AI chat panel (right), and the system responds with both textual answers and real-time updates to the 3D visualization (left). Python code executed in the integrated sandbox is shown in the console (bottom), providing full transparency and reproducibility of the underlying analyses.

chat panel and 3D molecular visualization capabilities (Figure 2 and Section 3.6). At its core is a Python sandbox powered by Pyodide, enabling the execution of Python code directly in the browser to manipulate structures and control the viewer. The sandbox includes a virtual file system, where structural files and related data are stored for visualization. Users interact through the chat panel, entering natural language

183 requests. The system interprets responses from the AI agent and parses them to display textual information  
 184 in the chat. It also detects when a specialized action is needed and invokes the corresponding viewer tools:  
 185

- 186 • **Virtual file system tool:** Loads required data files from the backend and stores them for visualization.
- 187 • **Python tool:** Executes Python code, as generated by the model, to carry out custom analyses or visual  
 188 manipulations.

190 The outputs from these tools are sent to the backend, which determines whether additional actions are  
 191 needed or if results should be presented in the user interface. The backend processes natural language  
 192 queries and orchestrates all available tools through a central AI agent, running either as a local LLM or via  
 193 an external API. Upon receiving a user request, the agent plans a sequence of actions, including complex  
 194 reasoning, modifying the viewer state, or invoking some of its domain-specific tools:

- 195 • **Literature Search:** Retrieves relevant scientific articles and extracts protein-related information from  
 196 PubMed Central.
- 197 • **UniProt Search:** Finds protein entries and annotations, including sequence, function, and cross-  
 198 references, from the UniProt database.
- 200 • **ChEMBL Search:** Retrieves bioactivity and assay data for small molecules and proteins from the  
 201 ChEMBL database.
- 202 • **PDB Search:** Locates experimental 3D structures and related metadata in the Protein Data Bank.
- 203 • **MoleculeKit Search:** Enables semantic search through the source code of MoleculeKit (Doerr et al.,  
 204 2016), a library for structure and formats manipulation.
- 205 • **A python sandbox.** Enables server-side computations using advanced libraries.

207 The system’s multimodal tooling layer is implemented as *Model Context Protocol (MCP)* (Anthropic, 2024)  
 208 servers that the model can invoke and compose during an interaction. Each tool provides a structured in-  
 209 terface to a core knowledge source, with outputs designed for integration into language reasoning and  
 210 context-conditioned retrieval-augmented generation (RAG). Concretely, we implement three primary tools:  
 211 (i) a literature retrieval component that performs sequence- and structure-grounded searches and builds a  
 212 protein-conditioned RAG corpus from PubMed Central; (ii) a UniProt interface that supports both accession  
 213 discovery and access to detailed entry information, including sequence data, cross-references, functional an-  
 214 notations, and literature links; and (iii) a ChEMBL interface for harvesting assay activities and surfacing  
 215 structure–activity relationship (SAR) information. All tools rely on programmatic access to public biologi-  
 216 cal databases and return normalized, machine-readable results, enabling the model to consistently connect  
 217 protein identity with structural, functional, and biochemical evidence. This modular organization allows  
 218 complex scientific queries to be decomposed into well-defined tool calls, whose implementation details we  
 219 describe in Sections 3.2–3.4.

## 220 3.2 LITERATURE SEARCH AND COMPREHENSION

222 The literature tool constructs a protein-specific corpus that can be searched with a text query. While the  
 223 literature discovery relies on *curated references from UniProt*, the tool can be invoked with either a UniProt  
 224 accession, PDB ID or FASTA sequence of the protein in question. If the user provides a UniProt accession,  
 225 the references linked to this entry are augmented by expanding the selection to all linked PDB structures.  
 226 If the input is a PDB code, the system first queries UniProt for all entries cross-referenced to that structure,  
 227 and then collects their reference lists. If the input is a raw FASTA sequence, the system searches the  
 228 Protein Data Bank to identify matching structures, resolves them to UniProt entries, and again retrieves  
 229 their references. This pathway ensures that the system always incorporates the expert-curated literature that  
 230 UniProt associates with a protein, regardless of the initial identifier type.

231 The result of the literature discovery step yields a diverse set of article identifiers, including PubMed IDs,  
 232 DOIs, and PubMed Central IDs. To unify them, we normalize all entries to *PubMed Central IDs (PMIDs)*  
 233 using a public conversion service. Importantly, only the subset of publications that are openly available  
 234 on PubMed Central can be downloaded and processed further; articles behind paywalls remain indexed  
 235 only by their identifiers. For each accessible PMID, we retrieve the article in XML format, which is  
 236 efficient to fetch and preserves section and paragraph boundaries. The text is cleaned and segmented into  
 237 coherent passages that are embedded into a vector space for retrieval-augmented generation (RAG) using  
 238 LlamaIndex (Liu, 2022).

239 All passages for a given protein are combined into a *protein-conditioned retrieval index*, together with  
 240 metadata such as PMID, DOI, and the set of matched PDB and UniProt identifiers (Table 2). The index  
 241 is cached on disk along with a list of associated protein identifiers (UniProt accessions, PDB IDs, FASTA  
 242 sequences), so future queries for the same target can reuse the corpus without repeated downloads. At  
 243 query time, the system formulates a descriptive retrieval prompt, retrieves the top- $k$  relevant passages,  
 and returns them along with their citations. The retrieved text is then provided to the language model

244 as grounded context, either to directly answer a user’s question (e.g., “Which mutations in CDK2 affect  
 245 inhibitor binding?”) or to supply background for further analysis and additional tool calls (e.g., filtering  
 246 ChEMBL assays for compounds tested in the cited studies, or highlighting reported residues in the 3D  
 247 structural viewer).

248 Despite involving multiple external databases and full-text retrieval, the entire pipeline runs in real time.  
 249 Literature discovery, download, and RAG construction typically complete within one to two minutes for a  
 250 new protein, and subsequent queries on the same target are handled within seconds due to caching of the  
 251 prebuilt index.

### 253 3.3 UNIPROT: ACCESSION DISCOVERY AND RICH ENTRY INFORMATION

255 The UniProt MCP server provides structured access to the UniProt knowledgebase, enabling both the dis-  
 256 covery of correct accessions and the retrieval of detailed entry information. It is organized into two comple-  
 257 mentary tools. The first is a text search utility that resolves canonical entries from colloquial protein names.  
 258 This call returns a concise shortlist with entry type, primary accession, protein name, organism, annotation  
 259 score, and keywords, allowing the model to select the most relevant entry—for example, the reviewed entry  
 260 of the correct organism—without inflating context.

261 Once an accession has been identified, the data lookup tool retrieves the corresponding UniProt record or  
 262 resolves from a PDB identifier when structures are the starting point. The response contains identifiers and  
 263 provenance suitable for citation, descriptive and gene fields, the full amino acid sequence, span-form fea-  
 264 tures encoding domains, active and binding sites, post-translational modifications, and variants, compressed  
 265 literature references with bibliographic fields and sequence “focus” positions, and a set of cross-references  
 266 that link the UniProt entry to other databases (Table 3). These include structural repositories such as the Pro-  
 267 tein Data Bank (PDB) and AlphaFoldDB, pharmacological resources such as DrugBank and DrugCentral,  
 268 and functional annotation databases such as Gene Ontology (GO). This representation is compact but ex-  
 269 pressive, preserving direct links to external resources while making it straightforward to highlight residues,  
 270 align sequences, or connect functional information across databases.

271 In practice, the model first issues a name query (when necessary), selects appropriate entries, and then  
 272 performs a data lookup to obtain a comprehensive record. The sequence can, for example, be forwarded  
 273 to the literature tool for protein-conditioned retrieval; feature spans can be used to create residue highlights  
 274 and distance measurements in the 3D viewer; and cross-references provide pivots to structures, pathways,  
 275 or pharmacology resources. The separation of discovery (name to accession) and enrichment (accession or  
 276 PDB to full entry) keeps tool contracts simple, enabling deterministic composition with other MCP servers.

### 277 3.4 CHEMBL: BIOACTIVITY AND SAR TABLES

279 The ChEMBL MCP server is dedicated to retrieving and organizing information about assays recorded  
 280 in the ChEMBL database. It focuses specifically on assay-level measurements of how molecules interact  
 281 with a given protein target. When invoked with a target identifier and an assay type, the tool downloads  
 282 all matching entries from the ChEMBL API to assemble a complete activity table. To reduce latency and  
 283 ensure reproducibility, the results are cached locally; repeated queries for the same target reuse this cache  
 284 until it expires.

285 Because raw ChEMBL activities are highly heterogeneous, mixing different units, redundant identifiers,  
 286 and free-text fields, the MCP normalizes the dataset into a streamlined representation that highlights the  
 287 essential biochemical information (Table 4). Rarely useful or inconsistent fields are removed, while values  
 288 necessary for reasoning about structure–activity relationships, such as standard measurements, molecule  
 289 identifiers, and publication context, are retained. All entries that pass this filtering are written to a tabular  
 290 file in CSV format. This file is stored on disk and its path is returned alongside a compact summary object.

291 The stored CSV file plays an important role in the overall system. It is directly accessible in the sandboxed  
 292 coding environment where the model can execute Python, enabling downstream analysis using libraries  
 293 such as pandas. For example, the model can reload the file, apply additional filters, calculate statistics, or  
 294 search for specific compounds that meet criteria relevant to the user’s query. This design separates the heavy  
 295 data retrieval and normalization step from the flexible, interactive analysis that happens later in dialogue  
 296 with the scientist.

297 For functional and binding assays, which are the most commonly used in drug discovery, the tool also high-  
 298 lights the most potent entries with standardized units. This provides a quick surface view of the strongest  
 299 bioactivity signals, while leaving the full dataset available for deeper inspection. Other assay families,  
 300 such as ADME or toxicity, are treated similarly but are generally provided only as complete CSV tables,  
 301 reflecting their diversity in format and measurement.

302 By structuring ChEMBL assay data into reproducible on-disk artifacts and linking them to a consistent sum-  
 303 mary interface, the MCP server makes assay information straightforward to query, analyze, and connect to  
 304 the other knowledge sources in the system. It allows the model to bridge from raw assay measurements

305 to literature and structural contexts, supporting seamless reasoning across biochemical, structural, and se-  
 306 quence evidence.  
 307

### 308 3.5 STRUCTURAL REPOSITORIES: PDB AND PREDICTED MODELS 309

310 The PDB MCP tool provides structured access to the Protein Data Bank (PDBe) API (Burley et al., 2018).  
 311 It can be invoked with one or more PDB identifiers to retrieve detailed entry information. This includes  
 312 metadata such as the experimental method, resolution, and publication details, as well as molecular infor-  
 313 mation like the list of co-crystallized small molecules (ligands). The tool automatically filters out common  
 314 solvents and ions to return only ligands relevant for analysis, providing their chemical identifiers (SMILES,  
 315 InChIKey) and cross-references to databases like ChEMBL (Table 5). This capability is crucial for large-  
 316 scale structural analyses, such as identifying all ligand-bound structures for a given protein target, a common  
 317 starting point in drug discovery projects.  
 318

### 319 3.6 MULTIMODAL GROUNDING AND INTERFACES WITH SCIENTISTS 320

321 Understanding proteins requires the navigation of multiple types of information, such as three-dimensional  
 322 structures, experimental assay tables, and textual annotations. A central goal of *Speak to a Protein* is to  
 323 connect these diverse modalities through a single conversational interface, ensuring that system responses  
 324 are not only generated in natural language but are also grounded in concrete evidence such as 3D visualiza-  
 325 tions, data tables, and executable code. To achieve this, we provide a set of interactive interfaces that extend  
 326 dialogue into complementary domains: a structural viewer for molecular inspection, a tabular analysis en-  
 327 vironment for filtering and plotting assay data, and mechanisms for synchronizing actions across views.  
 328 Together, these interfaces enable users to fluidly transition between asking questions, running analyses, and  
 329 visually verifying hypotheses. Significantly, we are building these capabilities on top of a web application  
 330 that has already attracted more than 18,000 registered users over the years, even in the absence of these AI  
 331 features. These new capabilities enable medicinal chemists with no-code experience to use the tools like an  
 332 expert computational chemist. We thus anticipate that it will be used by a considerable number of scientists,  
 333 as demonstrated by the platform usage metrics in Appendix A.3.  
 334

335 In *Speak to a Protein*, these functionalities are built using an entirely client-side sandbox for dynamic  
 336 visualization and manipulation of molecular structures (Torrens-Fontanals et al., 2024). The sandbox builds  
 337 on a browser-based molecular visualization toolkit that combines the high-performance mol\* visualization  
 338 engine (Sehnal et al., 2021), capable of rendering large biomolecular structures and molecular dynamics  
 339 trajectories directly in the browser, with a WebAssembly-enabled Python runtime (Pyodide). This allows  
 340 the use of powerful Python libraries such as MoleculeKit (Doerr et al., 2016) in the client environment,  
 341 enhancing the viewer’s capabilities to load and manipulate a wide range of common structural file formats,  
 342 from PDB and CIF to molecular dynamics trajectory files such as XTC and TRR.  
 343

344 A key feature is the ability to control this viewer through natural language commands. Requests such as  
 345 “highlight the ATP-binding site” are translated into tool calls that execute Python code within the viewer,  
 346 producing visual changes in real time (Fig. 2). Users can request a broad set of actions, such as:  
 347

- 348 • **Loading structures:** Users can instruct the system to load structures either from public sources or by  
 349 uploading custom files.
- 350 • **Controlling the visualization:** The AI can create, modify, or remove molecular representations on de-  
 351 mand. Structures or any of their subsets can be rendered in diverse styles, such as cartoon, ball-and-stick,  
 352 spacefill, or surface, and colored according to different properties, such as chain, residue type, secondary  
 353 structure, or user-defined colors. The selection logic uses the expressive VMD selection language, en-  
 354 abling complex queries like “show only the protein backbone,” “highlight tyrosine residues in chain A,”  
 355 or “display all residues within 5 Å of the ligand.”
- 356 • **Focusing the viewer:** The camera can be centered or zoomed onto regions of interest, such as active  
 357 sites, mutated residues, or selected domains.
- 358 • **Performing measurements:** Users can request measurements of distances, angles, or dihedrals between  
 359 atoms or residues.
- 360 • **Manipulating structures:** The system can modify loaded structures, for example, by filtering out water  
 361 molecules or other unwanted components, splitting chains, or extracting subsets for closer inspection.
- 362 • **Structural alignment:** Multiple structures can be superimposed based on selected atoms (e.g., C $\alpha$   
 363 atoms), allowing direct comparison of conformational states or homologous proteins.

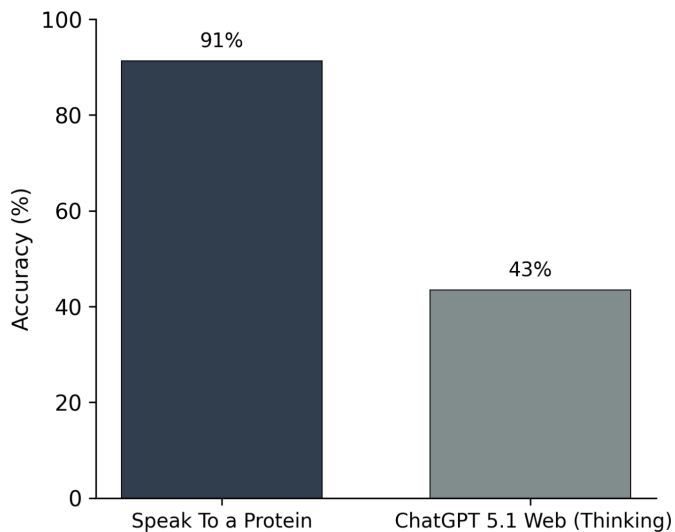
## 364 4 EXPERIMENTS 365

366 We present a set of illustrative case studies to show the capabilities and versatility of *Speak to a Protein*,  
 367 as well as a quantitative benchmark to validate its reliability on verifiable tasks. Firstly, we show, using  
 368

366 the dopamine D3 receptor (D3R) (Chien et al., 2010b) as a test case, the execution of a set of possible  
 367 questions that showcase the capabilities of the platform. These examples highlight how the system enables  
 368 users to ask scientific questions, integrate data from multiple sources, and rapidly generate insights through  
 369 multi-modal interactive analysis. Secondly, we ask a set of interactive questions on cyclin-dependent kinase  
 370 2 (CDK2) (Malumbres & Barbacid, 2009). Finally, we ask the AI to produce a summary report in LaTeX  
 371 of all the information gathered. By indexing all information, the system creates a knowledge base. Other  
 372 users can then interrogate it, knowing what is information model of the protein.

#### 374 4.1 QUANTITATIVE EVALUATION: BIO-STRUCTURAL BENCHMARK

375 We established a benchmark of 23 tasks designed to test capabilities essential for computational chem-  
 376 istry. The dataset spans four categories: (i) **Structural Geometry** (e.g., calculating RMSD, detecting steric  
 377 clashes, measuring residue distances); (ii) **Sequence Retrieval** (e.g., extracting specific chain sequences);  
 378 (iii) **Database Cross-Referencing** (e.g., retrieving ChEMBL potencies, identifying co-crystal ligands);  
 379 and (iv) **Literature Verification** (e.g., finding specific citations). We compared *Speak to a Protein* against  
 380 the standard **ChatGPT 5.1 Web (Thinking)**. This serves as a strong baseline as it is equipped with rea-  
 381 soning capabilities, web browsing, and a Python sandbox. However, it lacks the specialized biochemical  
 382 tools, a persistent virtual file system for cross-referencing API outputs, and the 3D visualization engine  
 383 integrated into our system. Tasks were scored strictly as correct or incorrect based on ground truth data  
 384 derived from programmatic calculation and database entries. As shown in Figure 3, *Speak to a Protein*



403 **Figure 3: Benchmark Performance.** Accuracy comparison between *Speak to a Protein* and the ChatGPT  
 404 5.1 Web (Thinking) on 23 curated bio-structural tasks.

406 achieved an accuracy of **91% (21/23)**, significantly outperforming the baseline at **43% (10/23)**. ChatGPT  
 407 5.1 frequently failed on tasks requiring precise structural geometry or specific bioactivity data. While it  
 408 represents a powerful general-purpose resource for scientists, it lacks the specialized infrastructure that  
 409 computational chemists require. Its reliance on web search often resulted in retrieval errors, and without  
 410 a specialized environment to manipulate and visualize molecular structures, it could not accurately derive  
 411 geometric properties. In contrast, our system succeeded by executing analysis scripts and querying domain  
 412 tools, ensuring that answers were derived directly from raw data and grounded in the interactive 3D viewer.  
 413 The full list of benchmark questions is provided in Appendix A.4.

#### 415 4.2 SPEAKING ABOUT THE DOPAMINE D3 RECEPTOR (D3R)

417 We use *Speak to a Protein* to address a series of research questions related to D3R, a G protein-coupled re-  
 418 ceptor of significant pharmacological interest. In the video trace <https://youtu.be/H6ag4JJAM0w>,  
 419 we show a possible user interaction with our system centered on D3R. The scientist begins by asking about  
 420 the available structures for this receptor, loading the listed structure 3PBL. Next, the user instructs the sys-  
 421 tem to filter for chain A, and changes the visual representation to focus on the binding pocket. Finally, it  
 422 requests a list of known inhibitors associated with D3R. All this information is collected and made available  
 423 to the AI so that knowledge is gathered and contextualized.

424 Focusing on the last query, we illustrate the workflow of the system (Figure 4). Upon the user’s request,  
 425 the AI used several tools in sequence to produce the necessary data. Using these tools, it identified the  
 426 correct UniProt entry for D3R and used it to query ChEMBL for all relevant bioactivity data. The retrieved  
 assay results were compiled and automatically stored in a CSV file, which was then loaded directly into the

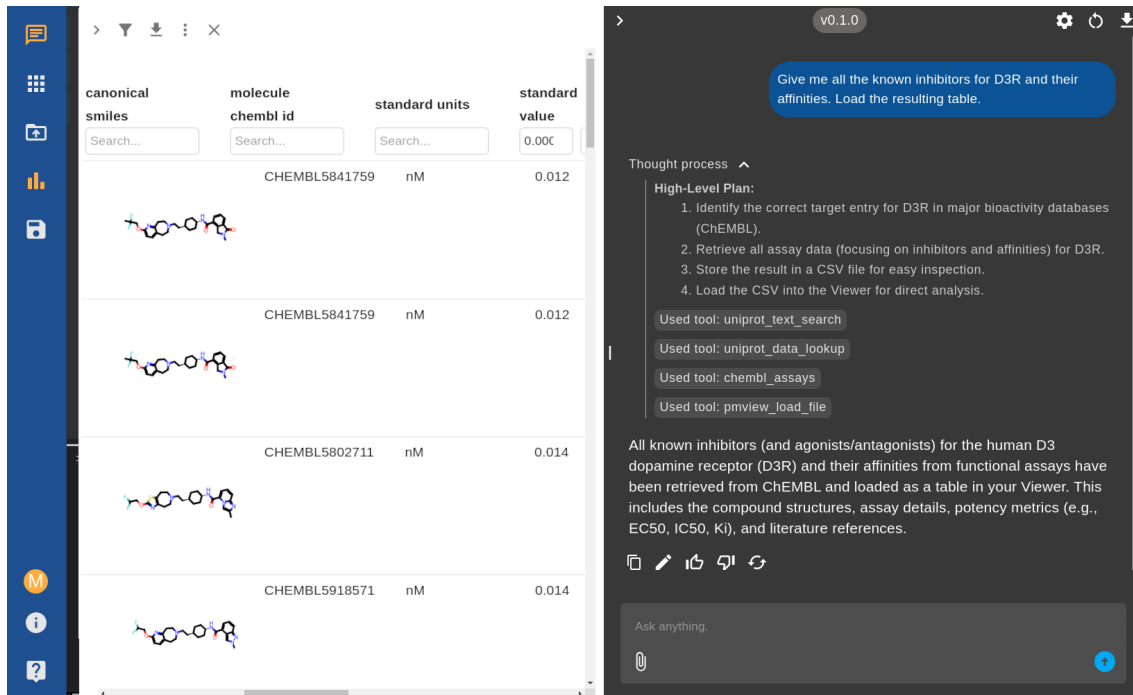


Figure 4: **Retrieval and exploration of potent D3R inhibitors.** Example user query and system workflow for fetching all known D3R inhibitors and their affinities using *Speak to a Protein*. The chat panel shows the AI’s reasoning, including the tools used and the final response. On the left, the interface displays an interactive table of D3R inhibitors, including chemical structures, ChEMBL IDs, assay details, and more, enabling direct exploration and further analysis.

viewer for exploration and analysis. The resulting table provides an overview of all known D3R inhibitors, along with chemical structures, assay details, potency metrics (such as EC50, IC50,  $K_i$ ), and references to the corresponding literature. Notable examples include inhibitors with subnanomolar to low nanomolar potencies such as CHEMBL5841759 ( $K_i$ : 0.012 nM) and CHEMBL5802711 ( $K_i$ : 0.014 nM). The results also listed several potent reference agonists for context.

In the video trace <https://youtu.be/nER3vC90ylQ>, we show how to investigate the differences between the D3 and D2 receptors. The literature search capability can help rapidly surface and synthesize expert knowledge from primary sources to address detailed structural questions. Upon receiving the prompt *“Based on the literature, compare the binding pockets of D3R and D2R and summarize the main structural features that could be exploited for ligand selectivity.”*, the system first uses *UniProt Search* to identify the canonical UniProt IDs for the specified proteins, ensuring precise target selection. Then, using *Literature Search*, an embedding-based literature search is performed, retrieving relevant articles and review information from PubMed Central that address the requested topic.

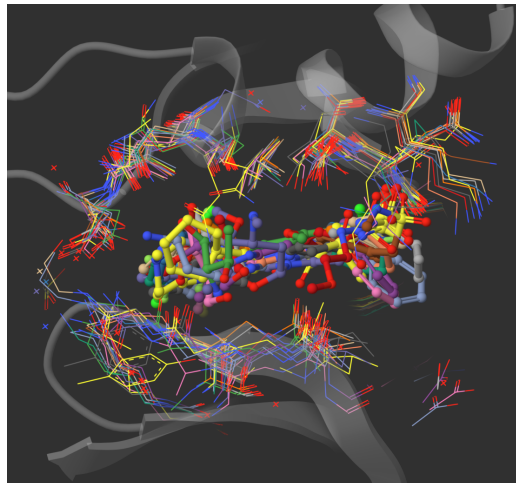
In this example, the system processed a set of 12 literature passages for D2R and 10 for D3R, selecting at least four distinct, peer-reviewed structural biology studies and related supporting works (Wang et al., 2018; Chien et al., 2010a; Yin et al., 2020; Fan et al., 2020). Based on this, the generated answer highlighted that while the orthosteric binding pocket is highly conserved, selectivity can be achieved by targeting differences in the architecture and flexibility of the ‘extended binding pocket’, as well as in the conformation of extracellular loops. It also described the significance of distinct residues (such as Trp100 and residues in EL1/EL2, positions 1.39 and 7.35) that shape ligand binding modes and selectivity opportunities. The resulting analysis revealed that while D3R and D2R share a conserved binding pocket core, D2R possesses additional flexible and hydrophobic residues that create a deeper, more accommodating pocket. These structural differences, clearly visualized and annotated in the viewer, help explain how each receptor achieves ligand selectivity, providing actionable insights for targeted drug design.

#### 4.3 SPEAKING ABOUT THE CYCLIN-DEPENDENT KINASE 2 (CDK2)

We present a complete drug discovery workflow using cyclin-dependent kinase 2 (CDK2), a validated cancer target with extensive structural and bioactivity data (Malumbres & Barbacid, 2009). This example showcases how *Speak to a Protein* can streamline the entire process from initial target evaluation to actionable insights. Our analysis begins with a systematic exploration of available structural data, progresses through mining and filtering of bioactivity data, and culminates in an integrated structural-activity analysis.

488  
489  
490  
491  
492  
493  
494  
495  
496  
497  
498  
499  
500  
501  
502  
503  
504  
505

pdb id	het id	name	smiles	chembl id
1 1AQ1	STU	STAUROSPORINE		CHEMBL388978
2 2A4L	RRC	R-ROSCOVITINE		CHEMBL14762
3 1OIT	HDT	4-[(4-IMIDAZO[1,2-A]PYRIDIN-3-YL)PYRIMIDIN-2-YLAMINO]BENZENESULFONAMIDE		CHEMBL73303
4 2W05	FRT	N-(2-METHOXYETHYL)-4-[(4-[2-METHYL-1-(1-METHYLETHYL)-1H-IMIDAZOL-5-YL]PYRIMIDIN-2-		CHEMBL478409



(a)

(b)

Figure 5: CDK2 structure–activity analysis. (a) Data integration and bioactivity analysis derived from ChEMBL datasets, demonstrating seamless integration of structural and bioactivity data through natural language queries. (b) Structural alignment of the top 20 most potent CDK2-ligand complexes with focused visualization of ATP-binding pockets.

The workflow highlights the system's ability to seamlessly transition between different data modalities and analysis types, all through natural language interactions.

**Structure-activity.** The complete conversational trace for this analysis is provided in the Appendix A.2. First, we ask the AI system to retrieve all available CDK2 structures from the Protein Data Bank. The system first used the UniProt tool to identify the canonical human CDK2 entry (P24941) and retrieve all 462 associated PDB structures. It then systematically queried each structure using the PDB information tool, which parsed each entry to extract co-crystallized ligands. After filtering out common solvents and ions, this process identified 479 unique ligand-structure pairs containing small molecules relevant for drug discovery. The system then automatically determined bioactivity coverage, revealing that 132 out of 258 ChEMBL-annotated ligands had experimental activity measurements available. Through systematic data cleaning and deduplication focused on  $IC_{50}$  values, we generated a refined dataset of approximately 100 unique CDK2-ligand complexes, ranked by potency. The top 20 most potent complexes ( $IC_{50}$  values ranging from sub-nanomolar to 15 nM) were loaded into the 3D viewer and structurally aligned (Figure 5). For detailed binding site analysis, the system identified and visualized only the ATP-binding pocket residues (within 6 Å of the co-crystallized ligands), excluding solvents and common crystallization agents.

**Automated Report Generation.** Furthermore, the AI extracted the binding pocket sequences and stored them in FASTA format. Pairwise sequence alignment revealed high conservation across the ATP-binding site, with only minor variations at peripheral positions. The AI system then conducted a comprehensive literature search to contextualize these findings with existing CDK2 research, automatically generating a markdown summary of relevant studies discussing binding site features and structure-activity relationships. The following report was automatically generated by the AI system, synthesizing all gathered data into actionable insights suitable for distribution to medicinal chemistry teams:

## CDK2 Structure-Activity & Binding Pocket Analysis

## Key Findings

**Structural Data Scope:** 462 unique CDK2 PDB structures identified and curated. 479 ligand/structure pairs contain co-crystallized non-solvent small molecules suitable for drug discovery.

**Bioactivity Integration:** 258 unique CDK2 co-crystallized ligands mapped to ChEMBL IDs. 132 ligands (51%) have direct annotated bioactivity data for CDK2 in public databases. After deduplication, 100 unique, potent (lowest IC<sub>50</sub>) ligand-structure matches represent the focused SAR set. Top 20 complexes span sub-nanomolar to low-nanomolar IC<sub>50</sub> values.

**Binding Pocket & Sequence Conservation:** The ATP-binding pocket is highly conserved across CDK2 structures, with the Gly-rich loop and DFG motif strictly maintained. Only minor sequence variations (G→V, Q/N, D/K) were observed at the pocket periphery. Pairwise sequence alignment scores are uniformly high, supporting a rigid, canonical scaffold for ligand engagement. All potent inhibitor binding modes overlay at this conserved

549 pocket, with activity cliffs mostly driven by ligand features rather than pocket sequence  
 550 variation.

551 *Structural Alignment & 3D Analysis:* 14 of the top 20 potent CDK2–inhibitor complex  
 552 structures were successfully aligned and visualized. Superposition reveals near-identity  
 553 of main pocket conformation but highlights loop and surface flexibility for ligand-induced  
 554 fit.

### 555 **Actionable Insights**

556 CDK2 displays a classic, highly druggable ATP-binding pocket with little sequence-  
 557 derived risk of resistance. SAR optimization should focus on maximizing hydrophobic  
 558 and hinge contacts, exploring diversity at the pocket periphery, and leveraging observed  
 559 loop conformational plasticity for next-gen analogs.

### 560 **Data Files Generated**

561 <b>Dataset Description</b>	562 <b>File</b>
563 PDB–ligand associations	564 <code>druglike_ligands.csv</code>
564 Annotated activity data	<code>ligands_annotated.csv</code>
565 IC <sub>50</sub> –focused dataset	<code>ligands_IC50_only.csv</code>
566 Deduplicated potency table	<code>ligands_dedup.csv</code>
567 Pocket sequences	<code>pocket_sequences.fasta</code>
Sequence alignments	<code>pocket_alignments.txt</code>
Literature synthesis	<code>literature_summary.md</code>

568 **Conclusion:** CDK2 remains a top-tier drug discovery target with a structurally robust,  
 569 deeply conserved and well-characterized ATP site optimal for inhibitor design—validated  
 570 by a wealth of crystal structures and directly observed SAR correlation.

571 The system’s ability to generate publication-ready reports and comprehensive literature summaries further  
 572 enhances its utility in collaborative drug discovery environments, where rapid communication of complex  
 573 structural and biochemical insights is essential for decision-making.

## 574 **5 CONCLUSION AND LIMITATIONS**

575 This study demonstrates how *Speak to a Protein* compresses traditional workflows involving several hours  
 576 of manual data gathering, analysis, and synthesis into an interactive session taking less than an hour. The  
 577 system’s ability to generate publication-ready reports further enhances its utility in collaborative drug dis-  
 578 covery environments where rapid understanding and communication of complex structural and biochemical  
 579 insights are essential for decision-making.

580 We found the following limitations in the current version of *Speak to a Protein*. The open web application  
 581 accesses only public information, such as literature, structure-activity relationships, and structural data.  
 582 This limits the data access and the understanding and downstream calculations. We plan to easily extend  
 583 it with additional tools to access internal or proprietary datasets, further broadening the scope of informa-  
 584 tion that can be queried, integrated. The 3D viewer can experience performance issues when rendering a  
 585 large number of complex structures simultaneously. We also observe occasional difficulties in seamlessly  
 586 connecting outputs between tools, stemming from different data representations across the system’s com-  
 587 ponents, e.g., residue indices across literature and structural databases. Furthermore, long tool outputs can  
 588 strain the model’s context window. Future work will focus on offloading large data payloads to files and  
 589 equipping the model with a broader set of tools for file management, allowing for more robust and complex  
 590 analytical workflows.

591 *Speak to a Protein* is freely accessible at <https://www.anonymousplayground.com>, which guar-  
 592 antees the reproducibility of the results shown.

## 593 **REFERENCES**

594 Anthropic. Introducing the Model Context Protocol, November 2024. URL <https://www.anthropic.com/news/model-context-protocol>.

595 Daniil A Boiko, Robert MacKnight, Ben Kline, and Gabe Gomes. Autonomous chemical research with  
 596 large language models. *Nature*, 624(7992):570–578, 2023.

597 Andres M. Bran, Sam Cox, Oliver Schilter, Carlo Baldassari, Andrew D. White, and Philippe Schwaller.  
 598 Augmenting large language models with chemistry tools. *Nature Machine Intelligence*, 6:525–535, 2024.  
 599 doi: 10.1038/s42256-024-00832-8.

600 Stephen K. Burley, Helen M. Berman, Cole Christie, Jose M. Duarte, Zukang Feng, John Westbrook,  
 601 Jasmine Young, and Christine Zardecki. Rcsb protein data bank: Sustaining a living digital data resource  
 602 that enables breakthroughs in scientific research and biomedical education. *Protein Science*, 27(1):316–  
 603 330, 2018. doi: <https://doi.org/10.1002/pro.3331>.

610 Davide Caffagni et al. The revolution of multimodal large language models: A survey. In *Findings of the*  
 611 *Association for Computational Linguistics: ACL 2024*, pp. 13590–13618, 2024.

612

613 Ellen Y.T. Chien, Wei Liu, Qiang Zhao, Vsevolod Katritch, Gye Won Han, Michael A. Hanson, Lei Shi,  
 614 Amy Hauck Newman, Jonathan A. Javitch, Vadim Cherezov, and Raymond C. Stevens. Structure of the  
 615 human dopamine d3 receptor in complex with a d2/d3 selective antagonist. *Science (New York, N.Y.)*,  
 616 330:1091, 11 2010a. ISSN 00368075. doi: 10.1126/SCIENCE.1197410. URL <https://pmc.ncbi.nlm.nih.gov/articles/PMC3058422/>.

617

618 Ellen YT Chien, Wei Liu, Qiang Zhao, Vsevolod Katritch, Gye Won Han, Michael A Hanson, Lei Shi,  
 619 Amy Hauck Newman, Jonathan A Javitch, Vadim Cherezov, et al. Structure of the human dopamine d3  
 620 receptor in complex with a d2/d3 selective antagonist. *Science*, 330(6007):1091–1095, 2010b.

621

622 S Doerr, M J Harvey, Frank Noé, and G De Fabritiis. Htmd: High-throughput molecular dynamics for  
 623 molecular discovery. *Journal of chemical theory and computation*, 12:1845–52, 4 2016. ISSN 1549-  
 624 9626. doi: 10.1021/acs.jctc.6b00049. URL <http://pubs.acs.org/doi/abs/10.1021/acs.jctc.6b00049>.

625

626 Luyu Fan, Liang Tan, Zhangcheng Chen, Jianzhong Qi, Fen Nie, Zhipu Luo, Jianjun Cheng, and Sheng  
 627 Wang. Haloperidol bound d2 dopamine receptor structure inspired the discovery of subtype selective lig-  
 628 ands. *Nature Communications*, 11:1074, 12 2020. ISSN 20411723. doi: 10.1038/S41467-020-14884-Y.  
 629 URL <https://pmc.ncbi.nlm.nih.gov/articles/PMC7044277/>.

630

631 Han Guo, Mingjia Huo, Ruiyi Zhang, and Pengtao Xie. Proteinchat: Towards achieving chatgpt-like  
 632 functionalities on protein 3d structures, 2023. URL <https://doi.org/10.36227/techrxiv.2312060>.

633

634 Alexander M Ille, Christopher Markosian, Stephen K Burley, Michael B Mathews, Renata Pasqualini, and  
 635 Wadih Arap. Generative artificial intelligence performs rudimentary structural biology modeling. *Sci-  
 636 entific reports*, 14(1):19372, 2024.

637

638 Hiroaki Kitano. Artificial intelligence to win a nobel prize and beyond: Creating the engine for scientific  
 639 discovery. *AI Magazine*, 42(1):39–51, 2021.

640

641 Namkyeong Lee, Edward De Brouwer, Ehsan Hajiramezanali, Tommaso Biancalani, Chanyoung Park,  
 642 and Gabriele Scalia. Rag-enhanced collaborative llm agents for drug discovery. *arXiv preprint  
 643 arXiv:2502.17506*, 2025. doi: 10.48550/arXiv.2502.17506. URL <https://arxiv.org/abs/2502.17506>.

644

645 Jerry Liu. LlamaIndex, 11 2022. URL [https://github.com/jerryjliu/llama\\_index](https://github.com/jerryjliu/llama_index).

646

647 Marcos Malumbres and Mariano Barbacid. Cell cycle, CDKs and cancer: a changing paradigm. *Nature  
 648 Reviews Cancer*, 9(3):153–166, 2009. doi: 10.1038/nrc2602.

649

650 David Mendez, Anna Gaulton, A Patrícia Bento, Jon Chambers, Marleen De Veij, Eloy Félix, María Paula  
 651 Magariños, Juan F Mosquera, Prudence Mutowo, Michał Nowotka, María Gordillo-Marañón, Fiona  
 652 Hunter, Laura Junco, Grace Mugumbate, Milagros Rodriguez-Lopez, Francis Atkinson, Nicolas Bosc,  
 653 Chris J Radoux, Aldo Segura-Cabrera, Anne Hersey, and Andrew R Leach. Chemb: towards direct  
 654 deposition of bioassay data. *Nucleic Acids Research*, 47(D1):D930–D940, 11 2018. ISSN 0305-1048.  
 655 doi: 10.1093/nar/gky1075. URL <https://doi.org/10.1093/nar/gky1075>.

656

657 Eric W Sayers, Jeffrey Beck, Evan E Bolton, Devon Bourexis, James R Brister, Kathi Canese, Donald C Comeau, Kathryn Funk, Sunghwan Kim, William Klimke, Aron Marchler-Bauer, Melissa Landrum, Stacy Lathrop, Zhiyong Lu, Thomas L Madden, Nuala O’Leary, Lon Phan, Sanjida H Rangwala, Valerie A Schneider, Yuri Skripchenko, Jiyao Wang, Jian Ye, Barton W Trawick, Kim D Pruitt, and Stephen T Sherry. Database resources of the national center for biotechnology information. *Nucleic Acids Research*, 49(D1):D10–D17, 10 2020. ISSN 0305-1048. doi: 10.1093/nar/gkaa892. URL <https://doi.org/10.1093/nar/gkaa892>.

658

659 David Sehnal, Sebastian Bittrich, Mandar Deshpande, Radka Svobodová, Karel Berka, Václav Bazgier,  
 660 Sameer Velankar, Stephen K Burley, Jaroslav Koča, and Alexander S Rose. Mol\* viewer: modern web  
 661 app for 3d visualization and analysis of large biomolecular structures. *Nucleic Acids Research*, 49:W431–  
 662 W437, 7 2021. ISSN 0305-1048. doi: 10.1093/NAR/GKAB314. URL <https://academic.oup.com/nar/article/49/W1/W431/6270780>.

663

664 Jinyuan Sun, Auston Li, Yifan Deng, and Jiabo Li. Chatmol copilot: An agent for molecular modeling  
 665 and computation powered by llms. In *Proceedings of the 1st Workshop on Language+ Molecules (L+ M  
 666 2024)*, pp. 55–65, 2024.

671 The UniProt Consortium. Uniprot: the universal protein knowledgebase in 2023. *Nucleic Acids Research*,  
672 51(D1):D523–D531, 11 2022. ISSN 0305-1048. doi: 10.1093/nar/gkac1052. URL <https://doi.org/10.1093/nar/gkac1052>.

673

674 Mariona Torrens-Fontanals, Panagiotis Tourlas, Stefan Doerr, and Gianni De Fabritiis. Playmolecule  
675 viewer: a toolkit for the visualization of molecules and other data. *Journal of Chemical Information  
676 and Modeling*, 64(3):584–589, 2024.

677

678 Chao Wang, Hehe Fan, Ruijie Quan, and Yi Yang. Protchatpt: Towards understanding proteins with  
679 large language models. *arXiv preprint arXiv:2402.09649*, 2024a. URL <https://arxiv.org/abs/2402.09649>.

680

681 H. Wang et al. Scientific large language models: A survey on biological & chemical domains. *arXiv  
682 preprint arXiv:2401.14656*, 2024b.

683

684 Sheng Wang, Tao Che, Anat Levit, Brian K. Shoichet, Daniel Wacker, and Bryan L. Roth. Structure of  
685 the d2 dopamine receptor bound to the atypical antipsychotic drug risperidone. *Nature*, 555:269, 3  
686 2018. ISSN 14764687. doi: 10.1038/NATURE25758. URL <https://pmc.ncbi.nlm.nih.gov/articles/PMC5843546/>.

687

688 Zhicong Wang, Zicheng Ma, Ziqiang Cao, Changlong Zhou, Jun Zhang, and Yiqin Gao. Prot2chat: Protein  
689 llm with early-fusion of text, sequence and structure. *arXiv preprint arXiv:2502.06846*, 2025.

690

691 Yijia Xiao, Edward Sun, Yiqiao Jin, Qifan Wang, and Wei Wang. Proteingpt: Multimodal llm for protein  
692 property prediction and structure understanding. *arXiv preprint arXiv:2408.11363*, 2024. URL <https://arxiv.org/abs/2408.11363>.

693

694 Jie Yin, Kuang Yui M. Chen, Mary J. Clark, Mahdi Hijazi, Punita Kumari, Xiao chen Bai, Roger K. Suna-  
695 hara, Patrick Barth, and Daniel M. Rosenbaum. Structure of a d2 dopamine receptor-g protein complex  
696 in a lipid membrane. *Nature*, 584:125, 8 2020. ISSN 14764687. doi: 10.1038/S41586-020-2379-5. URL  
697 <https://pmc.ncbi.nlm.nih.gov/articles/PMC7415663/>.

698

699 Y. Zhang et al. From automation to autonomy: A survey on large language models in scientific discovery.  
700 *arXiv preprint arXiv:2405.13259*, 2024.

701 Yunheng Zou, Austin H Cheng, Abdulrahman Aldossary, Jiaru Bai, Shi Xuan Leong, Jorge Arturo Campos-  
702 Gonzalez-Angulo, Changhyeok Choi, Cher Tian Ser, Gary Tom, Andrew Wang, et al. El agente: An  
703 autonomous agent for quantum chemistry. *Matter*, 8(7), 2025.

704

705

706

707

708

709

710

711

712

713

714

715

716

717

718

719

720

721

722

723

724

725

726

727

728

729

730

731

732 **A APPENDIX**  
733734 **A.1 TABLES**  
735736 Table 2: Fields returned by the Protein Literature MCP. Global fields describe the query context; results  
737 contain one or more retrieved citations with text passages.  
738

739	740	Field	Description / Example Value
741		fasta_sequences []	One or more FASTA sequences associated with the protein input.
742		pdb_ids []	PDB identifiers discovered for the input (via cross-references or sequence search). <i>Example</i> : [“1H1R”, “3DDQ”, “7RWE”]
743		uniprot_ids []	UniProt accessions associated with the input. <i>Example</i> : [“P24941”]
744		results [] .pmcid	PubMed Central ID for a retrieved article. <i>Example</i> : “PMC5291709”
745		results [] .doi	Digital Object Identifier for the article. <i>Example</i> : “10.7554/eLife.20818”
746		results [] .content	Retrieved text passage from the article body (cleaned paragraphs). <i>Example</i> : “ATP-binding sites involve Walker-A and -B motifs and a trigger residue that regulates hydrolysis.”
747		error	Error message if something went wrong; empty/absent otherwise. <i>Example</i> : “Failed to load existing RAG database: ...”
748			
749			
750			
751			
752			
753			
754			
755			
756			
757			
758			
759			
760			
761			
762			
763			
764			
765			
766			
767			
768			
769			
770			
771			
772			
773			
774			
775			
776			
777			
778			
779			
780			
781			
782			
783			
784			
785			
786			
787			
788			
789			
790			
791			
792			

793  
794  
795  
796  
797  
798  
799  
800

Table 3: Fields returned by the UniProt MCP. Two panels are shown: the upper panel lists fields from the **text search** tool (multiple candidate entries for a text query such as “CDK2”); the lower panel lists fields from the **data lookup** tool (detailed entries for a UniProt accession or PDB identifier).

Field (per entry)	Description / Example Value
<b>Panel A — Text search tool</b>	
entries[].entry_type	UniProt record type (reviewed/unreviewed).
entries[].uniprot_accession	Primary accession. <i>Example</i> : “P24941” (human CDK2).
entries[].knowledgebase_id	Human-readable ID. <i>Example</i> : [“CDK2_HUMAN”, “CDK2.MOUSE”].
entries[].name	Recommended, short and alternative protein names. <i>Example</i> : “Cyclin-dependent kinase 2”, “p33”, “Cell division protein kinase 2”.
entries[].organism	Common and scientific names. <i>Example</i> : “Human — Homo sapiens”.
entries[].annotation_score	Curation score string. <i>Example</i> : “5.0 out of 5”.
entries[].keywords[]	Keyword strings (category: name). <i>Example</i> : [“Ligand: ATP-binding”, “Molecular function: Kinase”]
<b>Panel B — Data lookup tool</b>	
primaryAccession	Canonical accession. <i>Example</i> : “P24941”.
uniProtkbId	Human-readable ID. <i>Example</i> : “CDK2_HUMAN”.
entryType	Record type (reviewed/unreviewed).
organism	Common and scientific names. <i>Example</i> : “Human — Homo sapiens”.
proteinDescription	Recommended full name and alternatives. <i>Example</i> : “Cyclin-dependent kinase 2”, alt: [“p33 protein kinase”].
genes[]	Gene symbols and synonyms. <i>Example</i> : [“CDK2”, “CDKN2”].
comments[]	Curated comment blocks (FUNCTION, SUBUNIT, PTM, ...). <i>Example</i> : FUNCTION describes CDK2 roles at G1/S.
features[]	Sequence features (“type   start:end”). <i>Example</i> : “Active site — 127:127”.
references[]	Bibliography (title, first author, date, journal, refs, focus).
crossref[]	External cross-refs as “Database:ID”. <i>Example</i> : [“PDB:1H1Q”, “DrugBank:DB07755”].
keywords[]	Structured keywords with category and name. <i>Example</i> : [“Molecular function: Kinase”].
sequence	Full amino acid sequence. <i>Example</i> : “MENF...HRL”.
annotationScore	Numerical annotation score. <i>Example</i> : 5.0.
proteinExistence	Evidence level. <i>Example</i> : “1: Evidence at protein level”.
secondaryAccessions[]	Secondary accessions, if any.
entryAudit	Versioning and dates. <i>Example</i> : first public 1992-03-01; last update 2025-06-18.
extraAttributes	Derived counts (comment/feature types) and UniParc ID.
error	Error message if something went wrong; empty otherwise.

850  
851  
852  
853

854  
 855  
 856  
 857  
 858  
 859  
 860  
 861  
 862  
 863  
 864  
**Table 4:** Fields returned by the ChEMBL MCP. Global fields describe the assay query context and where  
 865 results are stored; entries contain per-assay measurements with assay metadata, compound identifiers, and  
 866 activity values.  
 867

Field	Description / Example Value
assay_type	Type of assay retrieved from ChEMBL. <i>Example:</i> “functional”.
data_csv_path	File path on disk to the cached CSV table of results, available to the LLM in a sandboxed coding environment.
num_entries	Total number of entries returned by the query. <i>Example:</i> 927.
top_n	Number of top entries actually included in the response. <i>Example:</i> 20.
entries[].assay_chembl_id	ChEMBL identifier of the assay. <i>Example:</i> “CHEMBL663764”.
entries[].assay_description	Description of the assay protocol. <i>Example:</i> “Percentage A2780 cells in sub-G1 after 24 hr at 330 nM (IC50)”.
entries[].assay_type	Short assay type code. <i>Example:</i> “F”.
entries[].bao_label	BAO (BioAssay Ontology) label describing the assay format. <i>Example:</i> “cell-based format”.
entries[].molecule_chembl_id	ChEMBL identifier of the tested compound. <i>Example:</i> “CHEMBL428690”.
entries[].molecule_pref_name	Preferred molecule name, if available. <i>Example:</i> “ALVO-CIDIB”.
entries[].canonical_smiles	Canonical SMILES string of the compound.
entries[].document_chembl_id	Identifier of the source publication in ChEMBL. <i>Example:</i> “CHEMBL1135763”.
entries[].document_journal	Journal of publication (if known). <i>Example:</i> “J Med Chem”.
entries[].document_year	Year of publication (if known). <i>Example:</i> 2002.
entries[].standard_relation	Relation operator for the reported value. <i>Example:</i> “=”.
entries[].standard_type	Type of activity measured. <i>Example:</i> “Ki”, “Cell cycle”.
entries[].standard_units	Units of measurement. <i>Example:</i> “nM”.
entries[].standard_value	Reported numeric value. <i>Example:</i> “1.0”, “100.0”.

915 Table 5: Fields returned by the PDB MCP. The tool can fetch information for a single PDB ID or a list of  
 916 them. For a single ID, it returns a dictionary; for multiple, a list of dictionaries.  
 917

918 <b>Field</b>	919 <b>Description / Example Value</b>
920 <code>pdb_id</code>	PDB identifier. <i>Example:</i> "1AQ1"
921 <code>title</code>	Title of the PDB entry.
922 <code>experimental_method</code>	Experimental technique used. <i>Example:</i> "X-RAY DIFFRACTION"
923 <code>resolution_angstrom</code>	Resolution of the structure in angstroms. <i>Example:</i> 2.1
925 <code>publication_year</code>	Year of the primary publication.
927 <code>authors</code>	List of authors of the publication.
928 <code>journal</code>	Abbreviated journal name. <i>Example:</i> "Cell"
929 <code>doi</code>	Digital Object Identifier for the publication.
931 <code>deposit_date</code>	Date the structure was deposited.
932 <code>release_date</code>	Date the structure was released.
934 <code>small_molecules[]</code>	List of dictionaries, one for each co-crystallized small molecule ligand.
936 <code>small_molecules[] .het_id</code>	Heterogen ID of the ligand. <i>Example:</i> "STU"
937 <code>small_molecules[] .name</code>	Name of the ligand. <i>Example:</i> "STAUROSPORINE"
938 <code>small_molecules[] .smiles</code>	SMILES string of the ligand.
940 <code>small_molecules[] .inchi_key</code>	InChIKey of the ligand.
941 <code>small_molecules[] .chembl_id</code>	ChEMBL ID of the ligand, if available. <i>Example:</i> "CHEMBL388673"

## 945 A.2 FULL CONVERSATIONAL TRACE FOR CDK2 ANALYSIS

946  
 947 This section provides the complete, unedited conversational trace between the user and the *Speak to a  
 948 Protein* system for the CDK2 case study.

951 **User:** I'm starting a new research project focused on CDK2 (Cyclin-dependent kinase 2). Can you  
 952 retrieve all available PDB structures associated with CDK2?

955 **Assistant:** Great! Your goal is to get all available PDB structures for CDK2 (Cyclin-dependent  
 956 kinase 2). Here's the high-level plan:

### 957 **Checklist for Retrieving CDK2 PDB Structures**

- 959 1. Identify the correct UniProt accession code for human CDK2.
- 960 2. Cross-reference this accession with the PDB database to get all associated structures.
- 961 3. Provide you with the list of PDB IDs (optionally, titles or other metadata).

963 Let's start by finding the UniProt accession for human CDK2.

```
964 tool_execution: uniprot_text_search
965 tool_execution: uniprot_data_lookup
966 tool_execution: head
967 tool_execution: head
```

### 968 **Summary of Actions:**

- 969 • Identified the human CDK2 UniProt accession as P24941.
- 970 • Retrieved the cross-reference table of all PDB entries linked to this protein.
- 971 • Confirmed there are over 460 PDB structures associated with human CDK2.
- 972 • The first several PDB IDs include: 1AQ1, 1B38, 1B39, 1BUH, 1CKP, 1DI8, 1DM2,  
 973 1E1V, 1E1X, 1E9H, 1F5Q, 1FIN, 1FQ1, 1FVT, 1FVV, 1G5S, 1GIH, 1GII, 1GIJ.

976

977

978

979

980

981

982

983

984

985

986

987

988

989

990

991

992

993

994

995

**What's Next:** I can provide you with the full CSV containing all CDK2 PDB IDs for your research records, or perform further filtering (e.g., by resolution, ligand-bound states, etc.) if you have specific needs.

Would you like the complete list as a CSV download, or do you wish to explore/filter these structures further?

996

997

998

999

1000

1001

1002

1003

**User:** Great! Now I need to identify which of these CDK2 structures contain bound small molecules relevant for drug discovery. For each PDB structure with a co-crystallized small molecule ligand, please extract the ligand information, including the SMILES string and ChEMBL ID.

1004

1005

1006

1007

1008

1009

1010

1011

1012

1013

1014

1015

1016

1017

1018

1019

1020

1021

1022

1023

1024

1025

1026

1027

1028

1029

1030

1031

1032

1033

1034

1035

1036

```
tool_execution: run_python
tool_execution: pdb_info
tool_execution: run_python
tool_execution: pdb_info
tool_execution: head
tool_execution: run_python
```

All CDK2 PDB structures have been screened for co-crystallized small-molecule ligands, explicitly excluding common solvents and ions. Here's what was accomplished:

- A total of 462 CDK2 structures were checked.
- 479 unique ligand/structure pairs were identified that contain relevant small molecules suitable for drug discovery workflows (excluding water, ions, and common crystallization agents).
- For each entry, key information—PDB ID, ligand three-letter code, ligand name, SMILES string, and ChEMBL ID (when available)—has been extracted.

You can now download the structured CSV file with these results for your research: `cdk2_structures_with_druglike_ligands.csv`.

Do you want an overview table here, a full downloadable link, or further sub-filtering (e.g., by ligand/chemotype, ChEMBL presence, etc.)?

**User:** How many of our co-crystallized ligands now have annotated bioactivity data?

**Assistant:** Your question aims to determine how many of the CDK2 co-crystallized ligands identified (from the previous CSV, each with ChEMBL IDs when available) have associated, annotated bioactivity data.

Here's the high-level plan:

#### Checklist to Address Ligand Bioactivity Data

1. Extract the list of unique ChEMBL IDs among the co-crystallized ligands.
2. Query ChEMBL for bioactivity records for these ChEMBL IDs.
3. Count and report how many ligands have at least one bioactivity annotation.

Let's start by extracting the unique, non-null ChEMBL ligand IDs from the results file.

```
tool_execution: run_python
tool_execution: chembl_assays
tool_execution: run_python
tool_execution: head
```

1037

1038 tool\_execution: run\_python

1039

1040 **Result:** Out of 258 unique CDK2 co-crystallized small-molecule ligands with a ChEMBL ID, 132  
1041 have annotated bioactivity data in ChEMBL.

1042

1043 This means just over half of the ChEMBL-annotated ligands seen crystallographically with CDK2  
1044 have corresponding experimental activity measurements available—enabling robust structure-  
1045 activity relationship (SAR) and virtual screening workflows.

1046

1047 If you'd like, I can generate a CSV file listing all ligands with/without bioactivity data, or prioritize  
1048 by type/affinity ranges—just let me know your next analytic need!

1049

1050

1051 **User:** Excellent! Now let's load this dataframe into the viewer so I can explore and analyze the  
1052 data interactively.

1053

1054

1055

1056 **Assistant:** Perfect approach! Here's how we'll proceed:  
1057 **Checklist for Data Loading & Interactive Analysis**

1058

1059 

1. Prepare the relevant CSV with CDK2 PDB-ligand-activity data for the viewer.
2. Load the CSV into the Viewer's VFS (frontend).
3. Enable you to filter, sort, and explore SAR and ligand info interactively from the Viewer's  
1060 data table interface.

1061

1062 I will ensure the full co-crystal ligand dataset is loaded (with PDB ID, ligand name, SMILES,  
1063 ChEMBL ID, etc.), so you can immediately begin your exploration. The entire CDK2 struc-  
1064 ture-ligand dataset (including all PDB IDs, ligand names, SMILES, and ChEMBL IDs for co-  
1065 crystallized druglike compounds) is now loaded into the Viewer. You can interactively filter, sort,  
1066 and analyze the data directly in the viewer's table interface to support your structure-activity  
1067 relationship (SAR) and drug discovery workflows.

1068

1069 If you need to overlay additional columns, merge in the bioactivity values, or automate further  
1070 analyses, just let me know!

1071

1072 tool\_execution: pmview\_load\_file

1073

1074

pdb id	title	het id	name	smiles
1AQ1	HUMAN CYCLIN-DEPENDENT KINASE 2 COMPLEXED WITH THE INHIBITOR STAUROSPORIN E	STU	STAUROSPORINE	
1B38	HUMAN CYCLIN-DEPENDENT KINASE 2	ATP	ADENOSINE-5'-TRIPHOSPHATE	
1B39	HUMAN CYCLIN-DEPENDENT KINASE 2 PHOSPHORYLATED ON THR130	ATP	ADENOSINE-5'-TRIPHOSPHATE	
1OKP	HUMAN CYCLIN-DEPENDENT KINASE 2 COMPLEXED WITH THE INHIBITOR PURVALANOL B	PVB	PURVALANOL B	
1DQ8	THE STRUCTURE OF CYCLIN-DEPENDENT KINASE 2 COMPLEXED WITH THE INHIBITOR 4'DE-OH PURVALANOL B	DTQ	4'DE-OH PURVALANOL B	

**User:** Could you annotate the dataframe with the activity data for each compound?

1087

1088

1089 **Assistant:** Your goal is now to enrich the current dataframe—listing all CDK2 co-crystal lig-  
1090 ands—with their experimental activity data, where available. Here's the plan:

1091

1092 **Checklist for Activity Data Annotation**

1093

1094 

1. For each ligand in the dataframe (by ChEMBL ID), retrieve associated CDK2 bioactivity  
1095 values from ChEMBL.
2. Merge the experimental activity data (e.g.,  $IC_{50}$ ,  $K_i$ , units, assay type, etc.) into the original  
1096 structure-ligand CSV.
3. Reload the updated, annotated CSV into the viewer for interactive inspection.

1097

1098

1099

**Approach:**

1100

- I will extract activity records from the CDK2 ChEMBL assay CSV for all ChEMBL-mapped ligands in your PDB file.
- Merge these activity annotations back into the master ligand/PDB dataframe.
- Load the resulting enriched file for interactive SAR analysis.

1105

1106

1107

1108

Let's proceed with merging the activity data and preparing the annotated file. Your CDK2 co-crystal structure–ligand dataframe is now fully annotated with experimental activity data—including standard type ( $IC_{50}$ ,  $K_i$ , etc.), values, units, assay description, publication, and year—for each compound where available.

1109

1110

The annotated CSV is already loaded and ready for interactive sorting, filtering, and SAR analysis in the viewer.

1111

1112

If you want to visualize, group by, or further analyze any specific fields (e.g., color by  $IC_{50}$ , filter by activity type), just let me know your next analytic step!

1113

1114

```
tool_execution: run_python
tool_execution: pmview_load_file
```

1115

1116

1117

1118

1119

1120

1121

1122

pdb id	title	het id	name	smiles
1AQJ	HUMAN CYCLIN-DEPENDENT KINASE 2 COMPLEXED WITH THE INHIBITOR STAURSPORIN E	STU	STAURSPORIN E	
1838	HUMAN CYCLIN-DEPENDENT KINASE 2	ATP	ADENOSINE-5'-TRIPHOSPHATE	
1839	HUMAN CYCLIN-DEPENDENT KINASE 2 COMPLEXED WITH THE INHIBITOR PHOSPHORYLAT E ON THR 150	ATP	ADENOSINE-5'-TRIPHOSPHATE	
1OKP	HUMAN CYCLIN-DEPENDENT KINASE 2 COMPLEXED WITH THE INHIBITOR PURVALANOL B	PVB	PURVALANOL B	
1O9E	THE STRUCTURE OF CYCLIN-	OIQ	4-(2-HYDROXYXYLINOL O)O-	

**User:** The dataset looks comprehensive but has some redundancy. Let's clean it up by removing duplicate entries and focusing specifically on  $IC_{50}$  values, since these are the most commonly used and comparable activity measurements for structure-activity relationship analysis in drug discovery.

1133

1134

1135

1136

1137

1138

**Assistant:** Great—focusing on  $IC_{50}$  values and removing redundancy will streamline your SAR analysis. Here's the plan:

1139

**Checklist for Cleaning & Focusing the Dataset**

1140

1141

1142

1143

1144

1145

1146

1147

1148

1149

1150

1151

1152

1153

1154

1155

1156

1157

1158

I'll prepare the filtered file and update the viewer. The dataset has now been filtered to include only unique entries with experimentally measured  $IC_{50}$  values, the gold standard for SAR in drug discovery. Redundant rows have been removed, resulting in a concise dataset (353 unique records) now reloaded and ready for further interactive analysis in the Viewer.

If you want to further cluster by ligand, select only the best (lowest)  $IC_{50}$  per compound, or need additional summary statistics or visualizations, just let me know!

```
tool_execution: run_python
tool_execution: pmview_load_file
```





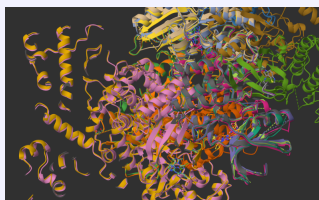
1281  
 1282     2. Remove all water molecules from every PDB structure (to declutter the binding pocket  
 1283        visualization).  
 1284     3. Ensure the ligand and relevant cofactors remain for clear analysis.

1285 Let's proceed to update all currently loaded structures as requested. All loaded CDK2 structures  
 1286 have been updated as follows:

1288     • Waters are removed from every complex.  
 1289     • Proteins are visualized in cartoon representation colored by structure-index, highlighting  
 1290        chain and domain diversity.  
 1291     • Ligands and cofactors remain, shown as ball-and-stick with element coloring.  
 1292     • Views are automatically focused on the protein for each structure.

1294 You can now clearly compare potent binding modes and structural features across your top com-  
 1295 plexes for SAR interpretation. Let me know if you'd like to further highlight specific residues,  
 1296 pocket regions, or overlay ligands!

1297 `tool_execution: pmview_run_python`



1301  
 1302     **User:** Now that all structures are loaded, please align them using  
 1303        structural superposition.  
 1304  
 1305  
 1306  
 1307  
 1308  
 1309  
 1310

1311     **Assistant:** Absolutely! Structural alignment (superposition) of all loaded CDK2 complexes will  
 1312        allow you to meaningfully compare the binding sites, conformational dynamics, and ligand posi-  
 1313        tioning across your top SAR hits.

#### 1314     **Checklist for CDK2 Structural Superposition**

1315     1. Select a reference CDK2 structure (e.g., the most potent or the first loaded structure).  
 1316     2. Align all other CDK2 protein chains to the reference using structural superposition (typi-  
 1317        cally on C atoms or the protein backbone).  
 1318     3. Update the visualization so that all complexes share the same spatial frame, facilitating  
 1319        pocket and ligand comparisons.

1320 I'll proceed by performing the superposition, using the protein backbone for robust alignment. It  
 1321 looks like the superposition function was not successfully imported, which suggests that superpo-  
 1322 sition might either need to be called differently or is located elsewhere in the library's API.

1323 To resolve this, I will search the library's codebase for the correct usage or import path for structural  
 1324 superposition/alignment and then apply the correct method to align all loaded CDK2 complexes.  
 1325 The library provides a built-in method for superposition:

- 1326     • Use the `align` method: `mol.align(sel, refmol, refsel)`
  - 1327        – `sel`: selection string for atoms to align (e.g., 'protein and backbone' or 'name CA')
  - 1328        – `refmol`: Molecule to align to (reference)
  - 1329        – `refsel`: atom selection for reference molecule (should match `sel` for structure-  
 1330        based alignment)

1331     Example usage (from documentation):

1332     `mol.align('protein', refmol=ref, refsel='protein')`

1333 This will superpose each molecule (`mol`) onto the reference (`ref`) using the selected atoms.

1334 I'll now perform this alignment for all currently loaded CDK2 structures using backbone atoms for  
 1335 maximal structural comparison. The alignment attempt failed due to differing numbers of backbone  
 1336 atoms between structures, which is common for PDBs with varying constructs, sequence bound-  
 1337 aries, or missing residues.

1338 To fix this, I'll use the library's `align` method with `mode='structure'`, which performs a struc-  
 1339 tural alignment regardless of atom order or counts, making it robust when sequence/atom mis-  
 1340 matches exist.

1342

1343

1344

1345

1346

Let's proceed with structure-based alignment for the superposition. All CDK2 complexes are now structurally aligned using robust structure-based superposition. This enables direct, meaningful comparison of binding modes, conformational variability, and ligand placement across your top potent co-crystal structures.

1347

1348

1349

You can now examine the aligned ensemble in the viewer for detailed SAR and structure-function insights. Let me know if you'd like to focus on active site residues, overplot specific ligands, or conduct further analyses!

1350

```
tool_execution: pmview_run_python
tool_execution: codebase_moleculekit_search
tool_execution: pmview_run_python
tool_execution: pmview_run_python
```

1354

1355

1356

1357

1358

1359

1360

1361

1362

1363

1364

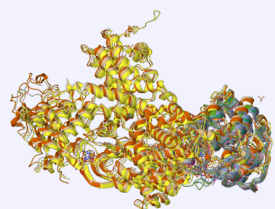
1365

1366

1367

1368

1369



**User:** Perfect! Now, for each structure, display only the ATP-binding pocket residues (within 6 Å of the ligand) and hide the rest of the protein.

1370

**Assistant:** Here's how we'll zoom in on the ATP-binding site for detailed analysis:

1371

1372

1373

1374

1375

1376

1. For each aligned CDK2 structure, identify all protein residues within 6 Å of the co-crystallized ligand.
2. Update the visualization to display only these ATP-pocket residues (hide all other parts of the protein).
3. Keep the co-crystallized ligand(s) visible with ball-and-stick representation.

1377

This will allow direct, uncluttered comparison of pocket residues and ligand interactions across all aligned complexes for SAR and binding analysis.

1378

Let's execute these selections and update your visualization accordingly. All aligned CDK2 structures are now focused solely on the ATP-binding pocket—showing only those protein residues within 6 Å of their co-crystallized ligand, together with the ligands themselves.

1380

This view enables you to directly compare key pocket residues and their interactions with high-potency ligands across the series, making SAR, hotspot, and mechanism-of-action assessments far more efficient.

1381

Let me know if you'd like to further highlight conserved residues, map mutations, overlay multiple ligands, or export pocket coordinates for computational analysis!

1382

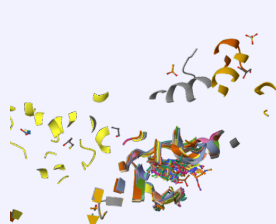
```
tool_execution: pmview_run_python
```

1383

1384

1385

1386



**User:** Do not consider solvents or ions like SO4, CH3, SGM, GOL, ACT, ACE as ligands for the pocket selection.

1387

1388

1389

1390

1391

1392

1393

1394

1395

1396

1397

1398

1399

1400

1401

1402

1403  
 1404 **Assistant:** Understood! For ATP-pocket residue selection, we'll strictly exclude all common crys-  
 1405 tallization agents, solvents, and ions—such as SO4, CH3, SGM, GOL, ACT, ACE, and others you  
 1406 listed. Only true organic/inhibitor ligands will define the selection.  
 1407

1408 **Checklist:**

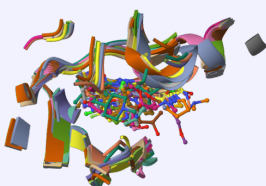
1. Exclude all common/solvent/ion three-letter codes from ligand identification.
2. For each structure, update the selection so the ATP pocket is defined by protein residues within 6 Å of only the remaining true ligand(s).
3. Keep only those pocket residues and the organic ligands visible.

1413 Let's refine the selections accordingly and update the viewer. All pocket views have now been  
 1414 refined: Only protein residues within 6 Å of true co-crystallized organic/inhibitor ligands are dis-  
 1415 played, strictly excluding all common solvents and ions (e.g., SO4, CH3, SGM, GOL, ACT, ACE,  
 1416 EDO, waters, metals). Ligands themselves remain clearly visible.

1417 You can now directly analyze the critical ATP-binding environments and ligand interactions across  
 1418 all top SAR cases—without any distracting non-relevant species.

1419 Let me know if you'd like to highlight conserved residues, compare ligand orientations, or export  
 1420 pocket coordinates for downstream modeling!

1421 `tool_execution: pmview_run_python`



1425 **User:** Could you extract the amino acid sequences of each of the  
 1426 binding pockets?

1435 **Assistant:** To extract the amino acid sequences of the ATP-binding pockets for each structure, we  
 1436 need to:

1437 **Checklist**

1. For each structure, identify all protein residues within 6 Å of the (properly filtered) lig-  
 and(s).
2. Retrieve the unique residue numbers and one-letter codes for these residues.
3. Output or save the binding pocket sequences (one per structure), which you can compare,  
 align, or analyze further.

1444 I will perform these steps and present the results in a tabular form for your review. You can use the  
 1445 library's `sequence` method, which has a selection argument (`sel`) to return the one-letter amino  
 1446 acid sequence for a given region, such as the ATP-binding pocket:

1447 Example usage:

1448 `pocket_sequence = mol.sequence(oneletter=True, sel=pocket_sel)`  
 1449 # Returns a dictionary: {segid: sequence}

1450 I'll apply this for each structure's identified pocket and display the resulting one-letter sequences  
 1451 for direct comparison. It appears there was an error when extracting the sequences—likely because,  
 1452 in some structures, the selected ATP pocket region is empty or not protein (e.g., no residues within  
 1453 6 Å, or the segment definition fails).

1454 To solve this, I'll adjust the script to handle cases with empty selections gracefully, so we can  
 1455 present the sequences for all successfully detected ATP pockets without failing on missing ones.  
 1456 Here are the ATP-binding pocket amino acid sequences (one-letter code, for residues within 6 Å of  
 1457 the filtered ligand) from each structure:

PDB ID	Pocket Sequence (one-letter code)
1aq1	IGEGTGVAKVFEFLHQDKPQNLLADL
3ddq	EKIGEGVKALKVFEFLHQDKQNLLEK...
1oit	IGEGGVVAKVFEFLHQDLKFQNLAD

```

1464
1465 | 2w05 | IGEGVAKVFEFLHQDLKFQNLAD
1466 | 2w17 | IGEVAKVFEFLHQDKKDQNLAD
1467 | 2vtp | IEGTGVVALKVFELHQDKQNLADL
1468 | 1r78 | IGEGETVVAVKVFELHQDKQNLADF
1469 | 3ns9 | EKIGEGTGVKALKVLFELHQDKQNLAD
1470 | 4bgh | IGEVAKVFEFLHQDLKFQNLAD
1471 | 2c6o | IEGTGVAKVFEFLHQDKFKQNLAD
1472 | 1ke6 | IGGVAKVFEFLHQDKQNLAD
1473 | 6gue | IGEYVAKEVFEFLHQDKQNLAD
1474 | 6gue | IEGETYVAKEVFEFLHQDLKQNLAD
1475 | 1ckp | EIVAKVFEFLHQDKQLAD
1476 | 1g5s | EIGEGTVKALKVFELHQDDKQNLAD
1477 | 2wpa | IGYVALKEVLFEFLHQDKKQNLADIGYV...
1478 | 1ke7 | IEGTYGVAKVFEFLHQDKFKQNLADL
1479 | 5iev | EIGEVALKVKFEFLHQDKFQNLAD
1480 | 2vu3 | IVVALKVFEFLHQDKQNLAD

```

1481 These sequences correspond to the local environment of the ATP site in each structure, capturing  
1482 subtle sequence or conformation differences. Let me know if you want these saved/downloadable,  
1483 aligned, or mapped onto your structures for further comparative analysis!

```

1484 tool_execution: pmview_run_python
1485 tool_execution: codebase_moleculekit_search
1486 tool_execution: pmview_run_python
1487 tool_execution: pmview_run_python
1488
1489
1490
1491

```

**User:** Thanks! Could you write them into a FASTA file?

**Assistant:** The ATP-binding pocket amino acid sequences for your CDK2 structures have been written into a single FASTA file:

`cdk2_pocket_sequences.fasta`

You can now download or use this file for sequence comparison, clustering, motif analysis, or further bioinformatics workflows. Let me know if you need a multiple sequence alignment or conservation analysis!

```

1501 tool_execution: run_python
1502
1503
1504
1505
1506
1507
1508
1509
1510
1511
1512
1513

```

**User:** Now please analyze the conservation patterns and sequence variations in these binding pocket sequences.

**Assistant:** Let's synthesize the insights from your ATP-pocket sequences and structural ensemble:  
**High-Level Analysis Plan**

1. Examine sequence conservation and variation across the ATP-binding pockets.
2. Relate observed patterns to ligand binding modes and measured activities.
3. Highlight any meaningful residue changes (substitutions, insertions, or deletions) and their possible structural/functional impacts on ligand binding.

### 1. Conservation Patterns

1514 Looking at your ATP-pocket FASTA sequences, there's strong conservation across the binding  
1515 site—the core motif `IGEGTGV(A/G)KVFEFLHQ(D/K)(K/Q)QNLAD(L/F)`—reflecting the  
1516 critical, evolutionarily fixed nature of the ATP site in CDK2.

1517 Most of the sequence changes are conservative (G→V, D→K, Q→N, etc.), clustered at the periphery, and rarely directly at residues known to contact ligands or substrate.

1525  
1526 **2. Key Sequence Variation Observations**  
1527

- 1528 • A few sites (notably G→V, D/K/Q exchanges) appear as minor variations across structures, with some longer sequences showing apparent repetition or possible unresolved loop insertions (e.g., in 3ddq or 2wpa).
- 1529 • The strong conservation of the “VFEFLHQD” region highlights its central role in ATP or inhibitor recognition; this is further supported by its near invariance in all structures.

1530  
1531 **3. Correlation with Binding Modes/Activities**  
1532

- 1533 • Because most potent ligands (lowest IC<sub>50</sub>) are co-crystallized with structures with identical or nearly identical pocket sequences, it reinforces that activity cliffs are driven more by ligand features and conformational fit than sidechain mutations in these structures.
- 1534 • Where variations exist at or near the pocket (e.g., E→Q or G→V), these changes may:
  - 1535 – Alter the shape or polarity/hydrophobicity of the local environment
  - 1536 – Induce repositioning of main/sidechains affecting direct or water-bridged hydrogen bonds, key for some ligand classes
  - 1537 – Potentially shift flexibility/“breathability” of the pocket size—favoring larger or more conformationally dynamic ligands

1538 If a specific structure’s ligand shows a marked difference in binding orientation (e.g., unique rotations, hydrogen bonding, or stacking), and that structure’s sequence has a rare variant in the pocket, this is a plausible hypothesis for the divergence in SAR.

1539 **4. Implications for Drug Design**  
1540

- 1541 • The deep conservation means CDK2 actives will likely recognize the same pocket features—the real SAR differentiation will be tied to microenvironments, local water networks, and dynamic sidechains.
- 1542 • Subtle variations (Q/N, D/K) could lead to favorable/unfavorable interactions for designed inhibitors, especially those with polar moieties.
- 1543 • For any observed outlier in binding mode or IC<sub>50</sub>, check if it coincides with an unusual local sequence change—it may be actionable for the next round of analog design.

1544 **Next Steps:**  
1545

- 1546 • I can generate a pairwise alignment or conservation plot for visual mapping.
- 1547 • If you’d like, I can map the sequence variations back onto your 3D structures for spatial correlation with ligand pose differences.

1548 Let me know your analytical or visualization preference for the next step!

1550 **User:** Generate a pairwise alignment.  
1551

1552 **Assistant:** A comprehensive pairwise alignment of all CDK2 ATP-pocket sequences has been  
1553 generated. Here’s what you can do next:

- 1554 • You can view the full file (all alignments, scores, and residue matches):  
1555 `cdk2_pocket_pairwise_alignments.txt`
- 1556 • The alignments quantify pairwise similarity (alignment scores) and precisely map where  
1557 insertions, deletions, or substitutions occur between each pocket.

1558 **Key Observations**  
1559

- 1560 • The core ATP-binding motif is highly conserved across nearly all your potent SAR structures.
- 1561 • Most pairwise similarity scores are high, with only rare single-residue or small motif deviations.
- 1562 • Insertions and rare longer repeats (e.g., in 3ddq, 2wpa) may reflect flexible loops or alternate segmentations, possibly influencing local conformational plasticity or ligand accommodation in outlier cases.

1563 **Practical Next Steps**  
1564

1586  
 1587     • Download and review the full alignment to correlate specific sequence changes with struc-  
 1588         tural or activity outliers.  
 1589     • Highlight in the viewer any pocket residues that vary in the pairwise alignments, for  
 1590         structure-guided design insights.

1592     If you'd like assistance visualizing the conservation or highlighting variable residues directly on  
 1593         your aligned 3D ensembles, I can guide you through that next!

1594     tool\_execution: run\_python

1595  
 1596  
 1597  
 1598     **User:** Based on our structural and sequence analysis findings, particularly the conservation pat-  
 1599         terns we identified and the sequence variations in the ATP-binding pocket, please search the litera-  
 1600         ture for CDK2 to find relevant studies that discuss these binding site features, structure-activity  
 1601         relationships, and any reported effects of pocket variations on inhibitor binding. This will help  
 1602         contextualize our findings with existing knowledge. Write this into a .md file  
 1603

1604  
 1605  
 1606     **Assistant:**

1607     tool\_execution: query\_protein\_literature  
 1608     tool\_execution: write\_file  
 1609     Your literature synthesis has been compiled into a markdown file:  
 1610     cdk2\_pocket\_literature\_summary.md.

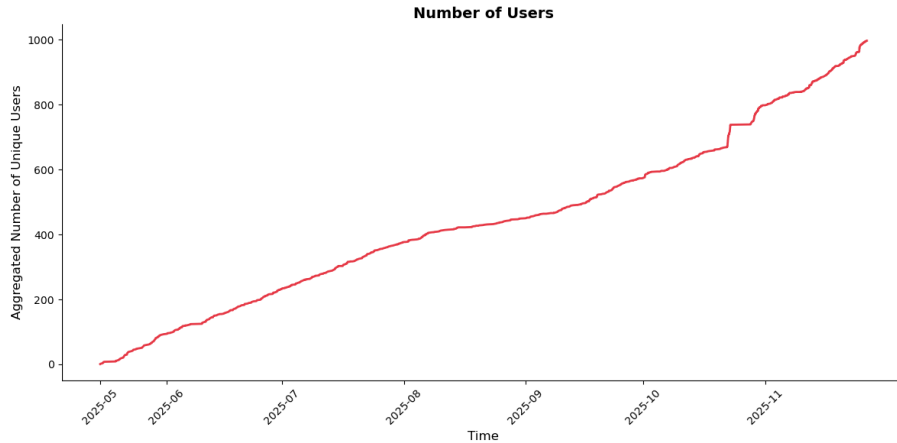
1611  
 1612     **User:** Based on our analysis, please generate a concise summary report for the head of chemistry.

1613  
 1614  
 1615  
 1616     **Assistant:**

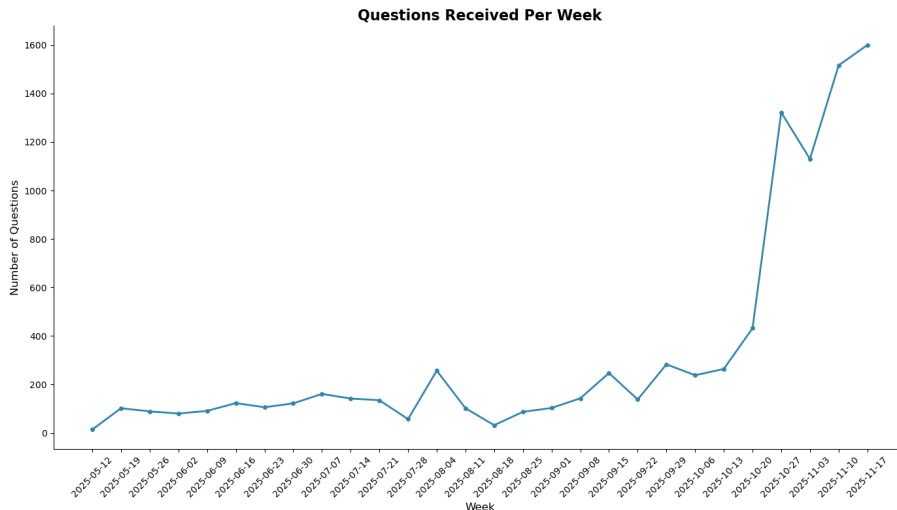
1617     tool\_execution: write\_file  
 1618     A concise executive summary for the head of chemistry has been prepared. You can download the  
 1619         report here: CDK2\_analysis\_summary.md.

1647 A.3 USAGE METRICS  
1648

1649 To demonstrate the practical utility and robustness of the system, we analyzed usage statistics from the  
1650 public deployment of *Speak to a Protein* between May 2025 and November 2025. These metrics reflect  
1651 organic adoption by the scientific community. As shown in Figure 6, the platform has seen consistent  
1652 growth in its user base. Simultaneously, the volume of interaction has accelerated. Figure 6b displays the  
1653 number of questions processed per week, which remained steady at approximately 100 queries/week during  
1654 the initial months and surged to over 700 queries/week by November.



(a) Aggregated number of unique users engaging with the AI Chat (May–Nov 2025).



(b) Weekly volume of natural language queries received by the system.

1690 **Figure 6: Platform Usage Statistics.** Usage metrics from the public release of *Speak to a Protein*, demon-  
1691 strating steady user adoption and a significant increase in query volume over the last six months.

1692  
1693  
1694  
1695  
1696  
1697  
1698  
1699  
1700  
1701  
1702  
1703  
1704  
1705  
1706  
1707

1708  
1709  
1710 A.4 BIO-STRUCTURAL BENCHMARK QUESTIONS  
17111712 We provide the full list of 23 questions used in the quantitative benchmark (Section 4.1). Results are  
1713 categorized as **Correct** or **Incorrect** (including incomplete or partially wrong answers). Tasks 1–12 focus  
1714 on structural queries and database retrieval, while tasks 13–23 include complex analysis, calculation, and  
1715 literature synthesis.1716 Table 6: Benchmark Tasks 1–12. Comparison of success rates on structural geometry and identification.  
1717

ID	Question	Speak To A Protein	ChatGPT 5.1 Web (Thinking)
1	For PDB 3L9H (Kinesin Spindle Protein), using the bound ligand EMQ as the reference, which protein residues have at least one atom within 6.0 Å of any EMQ atom? Return the residue list.	Correct	Incorrect
2	For PDB 1AQ1 (CDK2), using the bound inhibitor STU as the reference, which protein residues have at least one atom within 6.0 Å of STU? Return the residue list.	Correct	Incorrect
3	In PDB 1LYZ (lysozyme), what is the shortest O · · O distance (Å) between any side-chain carboxylate oxygen of Glu35 and any side-chain carboxylate oxygen of Asp52?	Correct	Incorrect
4	Using HIV-1 protease structures 1HHP (apo) and 1HVR (ligand-bound), align the proteins (backbone-based). After superposition, do any heavy atoms of the 1HVR ligand come within 2.0 Å of any heavy atom of flap residues 46–56 of 1HHP (i.e., a clash)?	Correct	Correct
5	For human CDK2, which residue must be phosphorylated for full kinase activation? Answer with residue name and number.	Correct	Correct
6	What is the primary ABL1 gatekeeper mutation associated with resistance to ATP-competitive inhibitors, and what is the corresponding residue name/number in PDB 2HYY?	Correct	Correct
7	What is the full amino acid sequence of chain A in PDB 1AQ1 (CDK2)? Return it in FASTA-style (header + sequence).	Correct	Correct
8	In PDB 1AQ1 (CDK2) with ligand STU, what is the shortest heavy-atom distance (Å) between any protein atom and any ligand atom?	Correct	Incorrect
9	For human EGFR, list compounds with $IC_{50} < 10$ nM. Provide at least 10 examples with: ChEMBL ID, name, $IC_{50}$ (nM), and SMILES.	Correct	Incorrect
10	Identify the 5 most potent human EGFR inhibitors by $IC_{50}$ (lowest, normalized to nM). Report if there is a PDB co-crystal structure of EGFR bound to that inhibitor, and list PDB IDs.	Correct	Incorrect
11	Find a PDB structure of influenza neuraminidase bound to oseltamivir (Tamiflu). What are the PDB ID and the reported resolution (Å)?	Correct	Incorrect
12	Identify a human dopamine D3 receptor (DRD3) co-crystal structure in the PDB. Report the PDB ID and the bound non-solvent small-molecule ligand.	Correct	Correct

Table 7: Benchmark Tasks 13–23. Comparison on complex analysis, calculation, and literature synthesis.

ID	Question	Speak To A Protein	ChatGPT 5.1 Web (Thinking)
13	From ChEMBL bioactivity data for human DRD3, retrieve $K_i$ measurements (nM). Provide a table of at least 20 entries with metadata (IDs, SMILES, assay/doc references).	Correct	Incorrect
14	Using CDK2 inhibitor complexes PDB 1AQ1 and 1H1Q, align 1H1Q onto 1AQ1 using protein C $\alpha$ atoms. What is the RMSD ( $\text{\AA}$ ) over the aligned C $\alpha$ atoms?	Correct	Incorrect
15	In PDB 1AQ1, list all non-protein hetero groups. Indicate which are solvents/ions vs. true ligand(s), and justify.	Correct	Correct
16	In PDB 3NY8, considering ligand CAU, list residues forming H-bonds, salt bridges, and hydrophobic contacts ( $\leq 4.0 \text{\AA}$ ). Report the count for each category.	Correct	Incorrect
17	How many distinct PDB structures are available for human CDK2 in the Protein Data Bank? Provide the count and description.	Correct	Correct
18	From ChEMBL, identify the 5 most potent CDK2 inhibitors by $IC_{50}$ (normalized to nM). Report values and compute their mean (nM).	Correct	Incorrect
19	For PDB 2HYY (ABL1), identify the bound non-solvent ligand(s). List protein residues within 6.0 $\text{\AA}$ (chain, name, number).	Correct	Incorrect
20	For the ligand in PDB 1HVR, compute RDKit-style descriptors: MW, cLogP, HBD, HBA, and TPSA.	Incorrect	Correct
21	Compare the binding-pocket size in PDB 3L9H (ligand EMQ) vs CDK2 PDB 1AQ1 (ligand STU). Which is larger and what quantitative proxy was used?	Incorrect	Incorrect
22	From structural literature on CDK2, which hinge-region residues are most commonly reported to form key H-bonds with inhibitors?	Correct	Correct
23	From structural literature comparing D3R and D2R, what binding-site features are reported to enable selective ligand design? Summarize and cite.	Correct	Correct